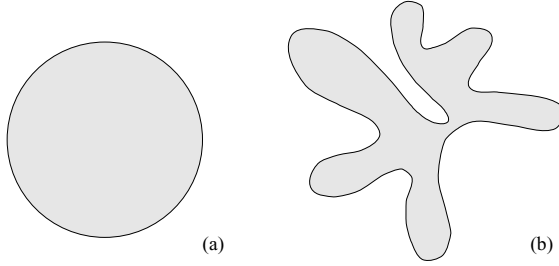


(see Section 6.2.3); using the outer boundary, compactness assumes values in the interval  $[16, \infty)$ . Independence from linear transformations is gained only if an outer boundary representation is used. Examples are shown in Figure 8.26.



**Figure 8.26:** Compactness: (a) compact; (b) non-compact. © Cengage Learning 2015.

### 8.3.2 Moments

Region moment representations interpret a normalized gray-level image function as a probability density of a 2D random variable. Properties of this random variable can be described using statistical characteristics—**moments** [Papoulis, 1991]. Assuming that non-zero pixel values represent regions, moments can be used for binary or gray-level region description. A moment of order  $(p + q)$  is dependent on scaling, translation, rotation, and even on gray-level transformations and is given by

$$m_{pq} = \int_{-\infty}^{\infty} \int_{-\infty}^{\infty} x^p y^q f(x, y) dx dy. \quad (8.41)$$

In digitized images we evaluate sums

$$m_{pq} = \sum_{i=-\infty}^{\infty} \sum_{j=-\infty}^{\infty} i^p j^q f(i, j), \quad (8.42)$$

where  $x, y, i, j$  are the region point co-ordinates (pixel co-ordinates in digitized images). Translation invariance can be achieved if we use the central moments

$$\mu_{pq} = \sum_{i=-\infty}^{\infty} \sum_{j=-\infty}^{\infty} (i - x_c)^p (j - y_c)^q f(i, j), \quad (8.43)$$

where  $x_c, y_c$  are the co-ordinates of the region's center of gravity (centroid), which can be obtained using:

$$x_c = \frac{m_{10}}{m_{00}}, \quad y_c = \frac{m_{01}}{m_{00}}. \quad (8.44)$$

In the binary case,  $m_{00}$  represents the region area (see equations 8.41 and 8.42). Scale-invariant features can be found from scaled central moments  $\eta_{pq}$  (scale change  $x' = \alpha x, y' = \alpha y$ )

$$\eta_{pq} = \frac{\mu_{pq}}{(\mu_{00})^{(p+q)/2+1}} \quad (8.45)$$

and normalized un-scaled central moments  $\vartheta_{pq}$

$$\vartheta_{pq} = \frac{\mu_{pq}}{(\mu_{00})^\gamma}. \quad (8.46)$$

Rotation invariance can be achieved if the co-ordinate system is chosen such that  $\mu_{11} = 0$  [Cash and Hatamian, 1987]. Many aspects of moment properties, normalization, descriptive power, sensitivity to noise, and computational cost are discussed in [Savini, 1988]. A less general form of invariance was given in [Hu, 1962] and is discussed in [Jain, 1989; Pratt, 1991], in which seven rotation-, translation-, and scale-invariant moment characteristics are used.

$$\varphi_1 = \vartheta_{20} + \vartheta_{02} , \quad (8.47)$$

$$\varphi_2 = (\vartheta_{20} - \vartheta_{02})^2 + 4 \vartheta_{11}^2 , \quad (8.48)$$

$$\varphi_3 = (\vartheta_{30} - 3 \vartheta_{12})^2 + (3 \vartheta_{21} - \vartheta_{03})^2 , \quad (8.49)$$

$$\varphi_4 = (\vartheta_{30} + \vartheta_{12})^2 + (\vartheta_{21} + \vartheta_{03})^2 , \quad (8.50)$$

$$\begin{aligned} \varphi_5 = & (\vartheta_{30} - 3 \vartheta_{12})(\vartheta_{30} + \vartheta_{12})((\vartheta_{30} + \vartheta_{12})^2 - 3(\vartheta_{21} + \vartheta_{03})^2) \\ & + (3 \vartheta_{21} - \vartheta_{03})(\vartheta_{21} + \vartheta_{03})(3(\vartheta_{30} + \vartheta_{12})^2 - (\vartheta_{21} + \vartheta_{03})^2) , \end{aligned} \quad (8.51)$$

$$\varphi_6 = (\vartheta_{20} - \vartheta_{02})((\vartheta_{30} + \vartheta_{12})^2 - (\vartheta_{21} + \vartheta_{03})^2) + 4 \vartheta_{11}(\vartheta_{30} + \vartheta_{12})(\vartheta_{21} + \vartheta_{03}) , \quad (8.52)$$

$$\begin{aligned} \varphi_7 = & (3 \vartheta_{21} - \vartheta_{03})(\vartheta_{30} + \vartheta_{12})((\vartheta_{30} + \vartheta_{12})^2 - 3(\vartheta_{21} + \vartheta_{03})^2) \\ & - (\vartheta_{30} - 3 \vartheta_{12})(\vartheta_{21} + \vartheta_{03})(3(\vartheta_{30} + \vartheta_{12})^2 - (\vartheta_{21} + \vartheta_{03})^2) , \end{aligned} \quad (8.53)$$

where the  $\vartheta_{pq}$  values can be computed from equation (8.46).

While these seven characteristics were shown to be useful, they are invariant only to translation, rotation, and scaling. Improved algorithms for fast computation of translation-, rotation-, and scale-invariant moments were given in [Li and Shen, 1991; Jiang and Bunke, 1991]. However, these do not yield descriptors that are invariant under general affine transforms. Details of a process for the derivation of invariants and examples of invariant moment object descriptions can be found in [Flusser and Suk, 1993], where a complete set of four affine moment invariants derived from second- and third-order moments is presented.

$$I_1 = \frac{\mu_{20} \mu_{02} - \mu_{11}^2}{\mu_{00}^4} , \quad (8.54)$$

$$I_2 = \frac{\mu_{30}^2 \mu_{03}^2 - 6 \mu_{30} \mu_{21} \mu_{12} \mu_{03} + 4 \mu_{30} \mu_{12}^3 + 4 \mu_{21}^3 \mu_{03} - 3 \mu_{21}^2 \mu_{12}^2}{\mu_{00}^{10}} , \quad (8.55)$$

$$I_3 = \frac{\mu_{20}(\mu_{21} \mu_{03} - \mu_{12}^2) - \mu_{11}(\mu_{30} \mu_{03} - \mu_{21} \mu_{12}) + \mu_{02}(\mu_{30} \mu_{12} - \mu_{21}^2)}{\mu_{00}^7} , \quad (8.56)$$

$$\begin{aligned} I_4 = & \left( \mu_{20}^3 \mu_{03}^2 - 6 \mu_{20}^2 \mu_{11} \mu_{12} \mu_{03} - 6 \mu_{20}^2 \mu_{02} \mu_{21} \mu_{03} + 9 \mu_{20}^2 \mu_{02} \mu_{12}^2 \right. \\ & + 12 \mu_{20} \mu_{11}^2 \mu_{21} \mu_{03} + 6 \mu_{20} \mu_{11} \mu_{02} \mu_{30} \mu_{03} - 18 \mu_{20} \mu_{11} \mu_{02} \mu_{21} \mu_{12} \\ & - 8 \mu_{11}^3 \mu_{30} \mu_{03} - 6 \mu_{20} \mu_{02}^2 \mu_{30} \mu_{12} + 9 \mu_{20} \mu_{02}^2 \mu_{21}^2 \\ & \left. + 12 \mu_{11}^2 \mu_{02} \mu_{30} \mu_{12} - 6 \mu_{11} \mu_{02}^2 \mu_{30} \mu_{21} + \mu_{02}^3 \mu_{30}^2 \right) / \mu_{00}^{11} . \end{aligned} \quad (8.57)$$

All moment characteristics are dependent on the linear gray-level transformations of regions; to describe region shape properties, we work with binary image data ( $f(i, j) = 1$  in region pixels) and dependence on the linear gray-level transform disappears.

Moment characteristics can be used in shape description even if the region is represented by its boundary. A closed boundary is characterized by an ordered sequence  $z(i)$

that represents the Euclidean distance between the centroid and all  $N$  boundary pixels of the digitized shape. No extra processing is required for shapes having spiral or concave contours. Translation-, rotation-, and scale-invariant one-dimensional normalized contour sequence moments  $\bar{m}_r, \bar{\mu}_r$  are defined in [Gupta and Srinath, 1987]. The  $r^{\text{th}}$  contour sequence moment  $m_r$  and the  $r^{\text{th}}$  central moment  $\mu_r$  can be estimated as

$$m_r = \frac{1}{N} \sum_{i=1}^N (z(i))^r, \quad (8.58)$$

$$\mu_r = \frac{1}{N} \sum_{i=1}^N (z(i) - m_1)^r. \quad (8.59)$$

The  $r^{\text{th}}$  normalized contour sequence moment  $\bar{m}_r$  and normalized central contour sequence moment  $\bar{\mu}_r$  are defined as

$$\bar{m}_r = \frac{m_r}{\mu_2^{r/2}} = \frac{\frac{1}{N} \sum_{i=1}^N (z(i))^r}{\left( \frac{1}{N} \sum_{i=1}^N (z(i) - m_1)^2 \right)^{r/2}}, \quad (8.60)$$

$$\bar{\mu}_r = \frac{\mu_r}{(\mu_2)^{r/2}} = \frac{\frac{1}{N} \sum_{i=1}^N (z(i) - m_1)^r}{\left( \frac{1}{N} \sum_{i=1}^N (z(i) - m_1)^2 \right)^{r/2}}. \quad (8.61)$$

While the set of invariant moments  $\bar{m}_r, \bar{\mu}_r$  can be used directly for shape representation, less noise-sensitive results can be obtained from [Gupta and Srinath, 1987]

$$F_1 = \frac{(\mu_2)^{1/2}}{m_1} = \frac{\left( \frac{1}{N} \sum_{i=1}^N (z(i) - m_1)^2 \right)^{1/2}}{\frac{1}{N} \sum_{i=1}^N z(i)}, \quad (8.62)$$

$$F_2 = \frac{\mu_3}{(\mu_2)^{3/2}} = \frac{\frac{1}{N} \sum_{i=1}^N (z(i) - m_1)^3}{\left( \frac{1}{N} \sum_{i=1}^N (z(i) - m_1)^2 \right)^{3/2}}, \quad (8.63)$$

$$F_3 = \frac{\mu_4}{(\mu_2)^2} = \frac{\frac{1}{N} \sum_{i=1}^N (z(i) - m_1)^4}{\left( \frac{1}{N} \sum_{i=1}^N (z(i) - m_1)^2 \right)^2}, \quad (8.64)$$

$$F_4 = \bar{\mu}_5. \quad (8.65)$$

Lower probabilities of error classification were obtained using contour sequence moments than area-based moments (equations 8.47–8.53) in a shape recognition test; also, contour sequence moments are less computationally demanding.

### 8.3.3 Convex hull

A region  $R$  is convex if and only if for any two points  $\mathbf{x}_1, \mathbf{x}_2 \in R$ , the whole line segment  $\mathbf{x}_1\mathbf{x}_2$  defined by its end points  $\mathbf{x}_1, \mathbf{x}_2$  is inside the region  $R$ . The convex hull of a region is the smallest convex region  $H$  which satisfies the condition  $R \subseteq H$ —see Figure 8.27. The convex hull has some special properties in digital data which do not exist in the continuous case. For instance, concave parts can appear and disappear in digital data